Turkish Journal of Physics

Volume 48 | Number 3 Article 4

2024

Comparative study of α-α interaction potentials constructed using various phenomenological models

AYUSHI AWASTHI

O S K S SASTRI

TÜBİTAK

Turkish Journal of Physics

http://journals.tubitak.gov.tr/physics/

Research Article

Turk J Phys
(2024) 48: 102 – 114

doi:10.55730/1300-0101.2760

Comparative study of α - α interaction potentials constructed using various phenomenological models

Ayushi AWASTHI, O. S. K. S. SASTRI*
Department of Physics and Astronomical Sciences, Central University of Himachal Pradesh
Dharamshala, Himachal Pradesh, Bharat, India

Received: 26.10.2023 • **Accepted/Published Online:** 09.04.2024 • **Final Version:** 13.06.2024

Abstract: In this paper, we have made a comparative study of $\alpha-\alpha$ scattering using different phenomenological models like Morse, double Gaussian, double Hulthén, Malfliet-Tjon, and double exponential for the nuclear interaction, and atomic Hulthén as the screened Coulomb potential. The phase equations for S, D, and G channels have been numerically solved using the 5^{th}-order Runge-Kutta method to compute scattering phase shifts (SPS) for the elastic scattering region consisting of energies up to 25.5 MeV. The model parameters in each of the chosen potentials were varied in an iterative fashion to minimize the mean absolute percentage error (MAPE) between simulated and expected SPS. A comparative analysis revealed that all the phenomenological models result in exactly similar optimized potentials with closely matching MAPE values for S, D, and G states. One can conclude that any mathematical function that can capture the basic features of two-body interaction will always guide the construction of optimized potentials correctly.

Key words: α -α scattering, phenomenological models, screened atomic Hulthén, scattering phase shifts, resonance energies

1. Introduction

Scattering studies of α particles with ^4_2He nuclei are important for understanding the nature of nuclear force and gaining insights into few-body [1] and cluster models [2, 3]. Rutherford and Chadwick were the first to study α-α scattering in 1927 [4] and since then, numerous experiments have been performed at various energy levels to deepen our understanding. In 1956, Heydenburg and Temmer presented experimental scattering phase shifts (SPS) for the low-energy range of 0.6 MeV to 3 MeV [5]. Tombrello and Senhouse, in 1963, provided experimental SPS covering the energy range of 3.84 MeV to 11.88 MeV [6]. Nilson et al., in 1958, reported SPS for energies between 12.3 MeV and 22.9 MeV [7]. Subsequently, Chien and Brown, in 1974, contributed experimental SPS for the energy range of 18 MeV to 29.50 MeV [8].

The SPS data obtained from these experiments were compiled by Afzal et al. [9], which is generally considered by theoretical physicists for studying $\alpha-\alpha$ scattering. However, it is worth noting that their compilation included data only up until 1969. Recognizing the significance of incorporating Chien and Brown data from 1974, Khachi et al. updated the database for α-α scattering in 2022 [10].

*Correspondence: sastri.osks@hpcu.ac.in

In the realm of theoretical physics, numerous phenomenological models have emerged and evolved over the past six decades. Notably, in 1964, Darriulat et al. [11] embarked upon a significant endeavor by employing the Woods-Saxon potential within an optical model. Their objective was to extract SPS for various angular momentum states, specifically $\ell = 0$, 2, 4, 6, and 8, spanning an energy range between 53 MeV and 120 MeV.

Almost at the same time, Ali and Bodmer ventured into the study of α-α scattering [12]. In their investigation, they employed a double Gaussian potential with four adjustable parameters. Their approach involved initially determining of the attractive component of the nuclear force by fitting the available scattering data in the $\ell = 4$ channel. Then, by constraining the shape of potential for large distances, they obtained the repulsive nature exhibited in the $\ell = 0$ and $\ell = 2$ channels at short distances.

In 1977, Buck et al. [13] put forth a compelling argument, emphasizing that a local potential is sufficient to model the interaction between α particles. They meticulously examined two notable models: the resonating group method [14] and the orthogonality condition model [15]. They employed a single Gaussian function characterized by two parameters obtained by selecting the experimental energy value of scattering state E = 0.0198 MeV and the phase shift for $\ell = 2$ at 3 MeV. They provided a reasonable explanation for the observed SPS for $\ell = 0$, 2, 4, and 6 for energy values up to $E_{\ell ab} =$ 80 MeV.

In 2003, Odsuren et al. combined two approaches, the complex scaling method and the orthogonality condition, to develop a method called CSOCM [16] to compute resonance states in two-body systems, considering the influence of Pauli exclusion principle between clusters. They applied two different potentials, Gaussian and harmonic oscillator, and obtained wave functions for the α-α system to calculate resonance energies along with their decay widths. In their calculations, they considered SPS for partial waves $\ell = 0$, 2, 4, 6, and 8, with energies up to 50 MeV.

Recently, Khachi et al. [17] revisited the local Gaussian potential using an innovative algorithm that combines the matrix method [18] with variational Monte Carlo [19] technique. In this approach, they considered the bound state energies as given in Buck et al. [13] to optimize the model parameters. Subsequently, by employing the determined interaction potential in the phase function method (PFM), they obtained SPS for $\ell = 0$, 2, and 4 channels for energies up to 25.5 MeV. Additionally, they proposed the Morse potential for the nuclear interaction and directly utilized all available experimental SPS to optimize the model parameters. This approach resembles constructing the model from the data, as in machine learning paradigm, which is fundamentally the approach of inverse scattering theory [20].

Another approach to investigate elastic α-α scattering involves employing ab initio techniques, specifically lattice Monte Carlo simulations. These simulations utilize lattice effective field theory to depict the low-energy interactions among protons and neutrons. Through the adiabatic projection method, the researchers reduced the complexity of the eight-body system to a two-cluster system. Their findings demonstrate encouraging concordance between lattice outcomes and experimental phase shifts observed in s-wave and d-wave scattering [21].In 2022, they refined their adiabatic projection method further, achieving a highly accurate depiction of S- and D-wave phase shifts at energies below 10 MeV in the chiral expansion at NNLO [22].

All of the procedures mentioned above [10, 12, 13, 16, 17] utilized the *erf()* function-based Coulomb interaction.

Alternatively, Laha et al. [23–25] utilized PFM to calculate SPS and obtain interaction potentials. They employed the double Hulthén potential to describe the nuclear interaction, while adopting the atomic Hulthén ansatz to account for the screened Coulomb interaction [26]. Their noteworthy study focused on investigating α-α scattering up to an energy range of $E_{\ell ab} = 100$ MeV. The motivation behind the present study was based on the following observations:

Firstly, we observed that for Morse + *erf()* ansatz of Khachi et al. [10], the depth of the potential for $\ell = 2$ is not shallower than that of $\ell = 0$. Therefore, we became intrigued to consider the performance of the atomic Hulthén screening potential as a replacement for *erf()*. This, in turn, led us to include a similar study for the double Gaussian potential [12].

Secondly, we observed that there were three studies [20, 23, 24] on α-α scattering using the double Hulthén potential as the nuclear interaction, with different screening radii. However, with those potential parameters, the height of the Coulomb barrier for $\ell = 2$ and 4 was not observed to be near their corresponding resonance energies [27]. Therefore, we opted to reoptimize the model parameters using our innovative algorithm within the elastic region, specifically up to 25.5 MeV.

Thirdly, the Malfliet-Tjon (MT) potential [28], which combines attractive and repulsive forms of the Yukawa potential [29], has been successful in reasonably explaining the SPS for n-p, n-d, and p-d systems [30]. Therefore,for the first time, we have incorporated this interaction potential to study α-α scattering.

Finally, an observation that the Morse potential is a composite of exponential functions has led us to incorporate the double exponential function into our analysis for the purpose of comparison.

Thus, in this paper, our aim is to perform a comprehensive comparative analysis of various phenomenological potential models as local potentials for modeling the nuclear interaction between two alpha particles. These models include the Morse, double Gaussian, double Hulthén, Malfliet-Tjon (MT), and double exponential. Our study focuses on investigating the elastic scattering of alpha particles (α-α) in the S, D, and G channels, utilizing the atomic Hulthén potential as the screened Coulomb potential for energies ranging up to 25.5 MeV.

2. Methodology

The interaction between two alpha particles is written as a combination of nuclear and Coulomb parts as follows:

$$V(r) = V_N(r) + V_C(r). \tag{2.1}$$

The nuclear part is modeled by various phenomenological potentials as follows:

- Morse potential [31]:

$$V_N(r) = D_0 \left(e^{-2(r-r_m)/a_m} - 2e^{-(r-r_m)/a_m} \right), \tag{2.2}$$

  where D_0 , r_m, and a_m represent the depth of the potential (in fm^{-2}), the equilibrium distance (in fm), and the shape of the potential (in fm), respectively. It is a three-parameter potential.

- Double Gaussian potential [12]:

$$V_N(r) = V_r e^{-\mu_r^2 r^2} - V_a e^{-\mu_a^2 r^2}, \tag{2.3}$$

where V_r and V_a represent the strength of the repulsive and attractive parts in fm^{-2}, respectively, μ_r and μ_a are their corresponding inverse ranges in fm^{-1}. It is a four-parameter potential.

- Double Hulthén potential [23]:

$$V_N(r) = -S_{\ell_1}\frac{e^{-\beta r}}{(e^{-\alpha r}-e^{-\beta r})} + S_{\ell_2}\frac{e^{-(\beta+\alpha)r}}{(e^{-\alpha r}-e^{-\beta r})^2}, \tag{2.4}$$

where S_{ℓ_1}, S_{ℓ_2}, α, and β are four parameters. The first two represent depth of the potential (in fm^{-2}) and the rest two its range (in fm^{-1}) of potential.

- Malfliet-Tjon (MT) potential [28]:

$$V_N(r) = \frac{V_R e^{-2\mu r} - V_A e^{-\mu r}}{r}, \tag{2.5}$$

where V_R and V_A represent depths of the repulsive and attractive parts of the potential in fm^{-2}, and μ is the inverse range parameter in fm^{-1}.

- Double exponential:

$$V_N(r) = Ae^{-\alpha_1 r} - Be^{-\alpha_2 r}, \tag{2.6}$$

where A and B represent depths of the repulsive and attractive parts of the potential in fm^{-2}, and α_1 and α_2 are inverse range parameters in fm^{-1}.

To account for the Coulomb interaction, we consider the atomic Hulthén potential [26] which is given as:

$$V_{AH}(r) = V_o\frac{e^{-r/a}}{(1-e^{-r/a})}, \tag{2.7}$$

where V_o is the strength of the potential and a is the screening radius. The two parameters V_o and a are related by [32]:

$$V_o a = 2K\eta,$$

where K is the momentum energy in lab frame and η is the Sommerfeld parameter defined as

$$\eta = \frac{\alpha}{\hbar v}.$$

Here, v is the relative velocity of the reactants at large separation and $\alpha = Z_1 Z_2 e^2$. Thus,

$$V_o a = \frac{Z_1 Z_2 e^2 \mu}{\hbar^2}.$$

For $\alpha-\alpha$, $Z_1 = Z_2 = 2$, $\mu = \frac{m_\alpha}{2} = 1864.38525\ \frac{MeV}{c^2}$, $e^2 = 1.44 MeV fm$ and therefore $V_o a = 0.2758 fm^{-1}$.

2.1. Phase function method

The time-independent Schrödinger equation (TISE) can be written as:

$$\frac{d^2u_\ell(r)}{dr^2} + \left[k^2 - \frac{\ell(\ell+1)}{r^2} - V(r)\right]u_\ell(r) = 0, \tag{2.8}$$

where $k_{c.m} = \sqrt{E_{c.m}/(\hbar^2/2\mu)}$ and $E_{c.m} = 0.5E_{\ell ab}$.

For the $\alpha - \alpha$ system, the value of $\hbar^2/2\mu = 10.44217$ MeVfm^2.

The phase function method is one an important tool in scattering studies for both local [33] and nonlocal interactions [34, 35]. The TISE in Eq.2.8 can been transformed to a nonlinear Riccati equation of first order [33, 37, 37], which directly deals with SPS information, given by:

$$\delta'_\ell(k,r) = -\frac{V(r)}{k}\left[\cos(\delta_\ell(k,r))\hat{j}_\ell(kr) - \sin(\delta_\ell(k,r))\hat{\eta}_\ell(kr)\right]^2. \tag{2.9}$$

The Riccati-Hankel function of first kind is given by: $\hat{h}_\ell(r) = -\hat{\eta}_\ell(r) + i\,\hat{j}_\ell(r)$, where $\hat{j}_\ell(kr)$ is Ricatti-Bessel and $\hat{\eta}_\ell(kr)$ Riccati-Neumann function. By substituting the expressions for different ℓ-values of these two later functions, we obtain the respective phase equations as:

1. $\ell = 0$:

$$\delta'_0(k,r) = -\frac{V(r)}{k}\sin^2[\delta_0 + \kappa] \tag{2.10}$$

2. $\ell = 2$:

$$\delta'_2(k,r) = -\frac{V(r)}{k}\left[-\sin(\delta_2+\kappa) - \frac{3\cos(\delta_2+\kappa)}{\kappa} + \frac{3\sin(\delta_2+\kappa)}{\kappa^2}\right]^2 \tag{2.11}$$

3. $\ell = 4$

$$\delta'_4(k,r) = -\frac{V(r)}{k}\left[\sin(\delta_4+\kappa) + \frac{10\cos(\delta_4+\kappa)}{\kappa} - \frac{45\sin(\delta_4+\kappa)}{\kappa^2} - \frac{105\cos(\delta_4+\kappa)}{\kappa^3} + \frac{105\sin(\delta_4+\kappa)}{\kappa^4}\right]^2 \tag{2.12}$$

where V(r) is the optimized potential defined in Eq. 2.1, with units of fm^{-2}. These equations are solved using 5th order Runge-Kutta methods by choosing the initial condition as $\delta_\ell(0,k) = 0$ and integrating to a large distance.

3. Results and discussion

The observed resonances in $\alpha - \alpha$ scattering experiments occurring at 0.09184 MeV, 3.03 MeV, and 11.35 MeV [38] corresponding to $\ell = 0$, 2, and 4 channels, respectively, provide an understanding of the ^8Be nuclear structure. These are named S, D, and G-states. The extremely strong resonance due to the S-state is attributed to the repulsive Coulomb interaction that introduces a barrier height and thus creates a resonance. Considering each of the potential models in the RK-5 algorithm for each

of the ℓ-channels, we have obtained corresponding best model parameters by minimizing the mean absolute percentage error (MAPE), given by:

$$MAPE = \frac{1}{N}\sum_{i=1}^{N}\left|\frac{\delta_i^{expected} - \delta_i^{simulated}}{\delta_i^{expected}}\right| \times 100, \tag{3.1}$$

where $\delta_i^{expected}$ and $\delta_i^{simulated}$ are the expected and simulated scattering phase shifts, respectively. This process of utilizing all the available experimental SPSs to determine the underlying interaction potential is akin to the procedure of inverse scattering theory. Thus, each of the phenomenological models are in effect proposing different mathematical functions that guide in constructing the optimized potential for various ℓ-channels [38].

Initially, we treated the screening radius a in the atomic Hulthén potential as a free parameter and obtained the optimized parameters by integrating the phase equation to a large distance of about 40 fm. This differs from the approach in ref. [10], where the erf() function was cutoff at about 6 fm to obtain the optimized parameters. The optimized parameters for $\ell = 0, 2$ along with their respective MAPE values are presented in Table 1. We did not present the optimized parameters for $\ell = 4$ because the number of experimental data points available for this channel is only 4, whereas the number of parameters in the case of double Hulthén, double Gaussian, and double exponential is 5. This implies that the number of equations to be solved is less than the number of unknowns, and the system is underdetermined. From Table 1, it is evident that the screening radius for $\ell = 0$ is greater than that for $\ell = 2$. Therefore, we conclude that as the angular momentum (ℓ) increases, the value of 'a' should decrease. One can observe that the MAPE converges to values between 1% and 2% for $\ell = 0$, and between 2% and 4% for $\ell = 2$. To plot the potential, we have rescaled the obtained V(r) by a factor of $\frac{\hbar^2}{2\mu}$ to express it in units of MeV. The potential plots for these two

Table 1. Model parameters of different mathematical functions for $\ell = 0$ and 2 with screening radius 'a' as free parameter.

Mathematical function model parameters	ℓ	Optimized parameters	Screening radius (a)	MAPE
Morse	0	(10.90, 3.31, 1.52)	4.77	1.5
(D_0, r_m, a_m)	2	(40.26, 2.02, 0.41)	3.31	2.0
Double Gaussian	0	(28.81, 97.46, 0.23, 0.51)	7.01	0.9
(V_a, V_r, μ_a, μ_r)	2	(193.58, 499.6, 0.58, 0.86)	3.55	2.4
Double Hulthén	0	(58.48, 44.35, 0.99, 0.36)	4.82	1.7
($S_{\ell 1}$, $S_{\ell 2}$, β, α)	2	(1623.35, 1494.35, 3.74, 2.07)	4.81	3.7
MT	0	(1335.69, 443.49, 0.50)	4.54	1.7
(V_R, V_A, μ)	2	(28771.21, 264.31, 1.54)	4.39	3.3
Double exponential	0	(78.65, 423.76, 1.22, 0.68)	4.69	1.4
(A, B, α_1, α_2)‘	2	(1994.15, 375.95, 3.07, 1.99)	4.13	3.1

channels without and with centrifugal term added are illustrated in Figures 1a and 1b, respectively. The inset of Figure 1a shows the centrifugal barrier height of $\ell = 0$ for various model potentials and it is observed that none of them are high enough to make the S-state to be a resonance. In Figure 1b, the inset shows the centrifugal barrier heights of $\ell = 2$, all of which vary from 2.5 to 3.5 MeV. Even though the barrier heights are close to 3 MeV as one would expect from the observed resonance of $\ell = 2$, the depths of the potential after adding the centrifugal term are not shallower than that of $\ell = 0$. All these observations made us realize that the optimized potentials are not physically realistic interactions. Hence, we have reoptimized the parameters to ensure that the following conditions are met:

1. The height of the Coulomb barrier for the S state is equal to or near the resonance energy.
2. When the centrifugal term is added, the potential depth for the D state is lower than that for the S state.
3. The heights of the Coulomb barrier for the D and G states are near their observed resonance energies respectively.

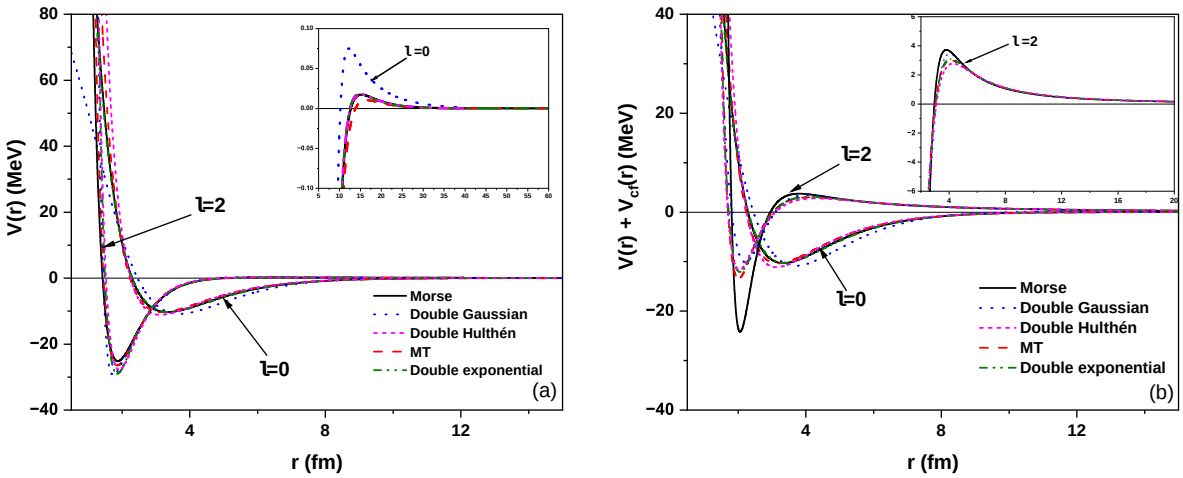

Figure 1. Interaction potential without and with centrifugal term $\ell = 0$ and 2.

In the second iteration, we chose various values of the screening radius 'a' and examined its impact on elucidating $\alpha - \alpha$ scattering. To achieve this, we began by increasing the a value and observed that the Coulomb barrier height kept increasing, as did the MAPE values. The obtained potential depth, barrier height, and corresponding MAPE values were compiled for values of a from 10 to 25 fm in steps of 5 fm for $\ell = 0$ S-state in Table 2. Overall, the trend is that while the depth of the potential decreases with increasing a, except for double Gaussian, the barrier height increases close to the expected 0.1 MeV. Similarly, for the D-state, a values were increased in steps of 1 fm from 4 fm onwards. It was found that up to 6 fm, the potential depth remained higher than that of the S-state, and only at 8 to 9 fm did the depths become shallower, except for the double exponential function. The barrier height keeps decreasing with increasing a, and the MAPE steadily increases as well. Finally, now that the screening parameter a is being fixed for a particular optimization run, we could obtain the parameters for $\ell = 4$ as well. It was observed that for higher ℓ values, the screening parameter

reduces. Hence, the values of a were started at an even smaller value and more fine tuned by varying only in steps of 0.5 fm now, from 3 to 4.5 fm. The barrier height keeps decreasing with increasing screening radius as in the case of D-state. On the other hand, MAPE values tend to decrease for MT and double Hulthén, increase in the case of double Gaussian, and reach a minimum in the cases of Morse and double exponential for some in between a values. While the double exponential gives the best MAPE of 0.1 at a = 4fm, Morse has the best value of 0.5 at 3.5 fm. One can choose different sets of a values for each of the 5 model potentials as given in Table 3 and compare the respective interaction potentials for S, D, and G states.

Table 2. Potential depth, barrier height, and MAPE at different screening radius ('a') for $\ell = 0$, 2, and 4.

$\ell = 0$				
MF/a	10fm	15fm	20fm	25fm
Morse	[-10.85, 0.07, 1.6]	[-10.43, 0.09, 1.6]	[-10.37, 0.11, 1.6]	[-10.28, 0.11, 1.6]
Double Gaussian	[-11.32, 0.11, 0.8]	[-11.84, 0.14, 0.9]	[-12.07, 0.16, 0.9]	[-12.17, 0.17, 0.9]
Double Hulthén	[-11.23, 0.06, 1.8]	[-11.33, 0.09, 1.8]	[-11.52, 0.11, 2.1]	[-11.50, 0.12, 2.1]
MT	[-10.95, 0.06, 1.7]	[-10.23, 0.08, 1.7]	[-10.09, 0.09, 1.7]	[-9.95, 0.10, 1.6]
Double exponential	[-10.73, 0.07, 1.4]	[-10.46, 0.09, 1.5]	[-10.40, 0.11, 1.5]	[-10.51, 0.13, 1.5]
$\ell = 2$				
MF/a	6fm	7fm	8fm	9fm
Morse	[-10.82, 2.81, 3.8]	[-9.56, 2.69, 4.3]	[-8.82, 2.63, 4.5]	[-8.51, 2.56, 4.3]
Double Gaussian	[-12.98, 2.96, 4.2]	[-11.28, 2.87, 4.6]	[-10.23, 2.82, 4.9]	[-10.08, 2.78, 5.2]
Double Hulthén	[-11.77, 2.74, 3.8]	[-10.75, 2.63, 4.3]	[-10.04, 2.55, 4.6]	[-9.59, 2.49, 4.8]
MT	[-11.85, 2.85, 3.8]	[-10.56, 2.69, 4.2]	[-9.80, 2.61, 4.5]	[-9.34, 2.55, 4.7]
Double exponential	[-14.29, 2.81, 3.7]	[-13.53, 2.68, 4.2]	[-11.77, 2.60 ,4.6]	[-11.57, 2.55, 4.7]
$\ell = 4$				
MF/a	3fm	3.5fm	4fm	5fm
Morse	[-0.02, 10.98, 1.3]	[0.06, 10.80, 0.5]	[0.06, 10.67, 0.7]	[0.06, 10.44, 1.2]
Double Gaussian	[0.13, 9.79, 2.7]	[0.13, 9.61, 3.3]	[0.13, 9.53, 3.8]	[0.13, 9.32, 4.6]
Double Hulthén	[-2.67, 11.56, 3.7]	[-1.83, 11.37, 2.9]	[-1.11, 11.22, 2.3]	[0.13, 10.95, 1.2]
MT	[-3.13, 11.59, 3.4]	[-2.312, 11.40, 2.6]	[-1.61, 11.24, 2.0]	[-0.27, 10.95, 1.1]
Double exponential	[0.03, 10.74, 0.7]	[0.03, 10.67, 0.4]	[0.03, 10.71, 0.1]	[0.03, 10.56, 1.1]

The interaction potentials, with and without the centrifugal term, is depicted in Figure 2. From the inset of Figure 2a, it is evident that resonance energy for $\ell = 0$ are obtained for all phenomenological models. Additionally, Figure 2b reveals that the inclusion of the centrifugal term causes the depth of the potential to be lower for $\ell = 2$ and 4 compared to $\ell = 0$, for all models except the double exponential model. Based on all these comparative observations, one can easily observe that the optimized potentials obtained using any of the chosen mathematical models are nearly identical, with negligible variations, as they all converge to give mean absolute percentage errors within about 1%. Therefore, even though many different mathematical functions have been proposed over the years, they all guide the process of constructing optimized potentials in exactly the same manner.

Table 3. Optimized model parameters of different mathematical functions for $\ell = 0$, 2, and 4. The screening radius 'a' is shown in bold.

Mathematical function	Model parameters	ℓ =0	ℓ=2	ℓ=4
Morse	(D_0, r_m, a_m, **a**)	(11.18, 3.42, 1,63, **15.0**)	(27.06, 1.89, 0.63, **7.0**)	(241.66, 0.37, 0.74, **3.5**)
	MAPE	1.6	4.3	0.5
Double Gaussian	(V_a, V_r, μ_a, μ_r, **a**)	(42.79, 98.36, 0.24, 0.44, **20.0**)	(68.93 , 36102.08, 0.48, 1.78, **8.0**)	(128.68, 1.24, 0.49, 4.46 , **0.5**)
	MAPE	0.9	4.6	0.5
Double Hulthén	($S_{\ell 1}$, $S_{\ell 2}$, β, α, **a**)	(48.54, 35.67, 1.49, 0.90, **15.0**)	(1065.54, 963.88, 2.10, 0.54, **7.0**)	(48.17, 1.33, 5.36, 4.14, **5.0**)
	MAPE	1.9	4.3	1.2
MT	(V_R, V_A, μ, **a**)	(1080.63, 408.32, 0.43, **20.0**)	(8284,89, 1330.72, 1.27, **8.0**)	(958.32, 857.18, 1.01, **5.0**)
	MAPE	1.7	4.5	1.1
Double exponential	(A, B, α_1, α_2, **a**)	(117.14 , 80.59, 0.89, 0.73, **25.0**)	(8597.48, 52.55, 4.86, 1.39, **9.0**)	(55.51, 68.62, 3.08, 1.32, **4.0**)
	MAPE	1.5	4.7	0.1

One might think that this might be due to global optimization algorithm which seems to always converge to similar shape for the optimized potentials. Therefore, to test this, we have considered only as many experimental data points as per the number of model parameters so that the equations are neither underdetermined nor overdetermined. That is, we have obtained interaction potentials, for three-parameter Morse and MT potentials, by considering the following energies for each of the partial waves during optimization:

1. $\ell = 0$: E=[0.85 MeV, 9.88 MeV, 25.55 MeV]
2. $\ell = 2$: E=[3.84 MeV, 7.47 MeV, 25.55 MeV]
3. $\ell = 4$: E=[18 MeV, 21.13 MeV, 25.55 MeV]

Similarly, for mathematical functions with four parameters, such as double Gaussian, double Hulthén, and double exponential potentials, we have extended our analysis by adding one additional energy point for each ℓ value, which are $2.5MeV, 18MeV, 24.11MeV$ for $\ell = 0$, 2, and 4, respectively. The obtained parameters for S, D, and G-states considering each model potential are compiled in Table 4. It is evident that the results are comparable to those obtained from the global optimizations algorithm. Even the mean absolute percentage errors obtained are only slightly higher than those obtained using GOA.

The obtained SPS for S, D, and G states are shown in Figure 3. They follow the same trend as the expected ones [10] for $\ell = 0$ and 4. However, there are slight discrepancies from a lab energy of 7.88 MeV to 11.88 MeV for $\ell = 2$. Therefore, we can conclude that the atomic Hulthén as a screened Coulomb potential works well for the S and G states, but it is not as effective in capturing the peak that appears in the SPS of the D state, when we use phase function method to calculate SPS. One can also conclude that all the mathematical functions are more or less equally effective in guiding the construction of optimized potentials for all the ℓ-channels.

Table 4. Optimized Model parameters of interaction potential for $\ell = 0$, 2, and 4 by taking number of data points equal to the number of model parameters.

Mathematical function	Model parameters	ℓ =0	ℓ=2	ℓ=4
Morse	(D_0, r_m, a_m, **a**)	(11.46, 3.35, 1.58, 15.0)	(27.04, 1.92, 0.62, 7.0)	(214.16, 0.47, 0.73, 3.5)
	MAPE	2.3	4.5	1.0
Double Gaussian	(V_a, V_r, μ_a, μ_r, **a**)	(50.77, 100.42, 0.24, 0.41, 20.0)	(53.97, 15558.85, 0.45, 1.80, 8.0)	(128.68, 1.24, 0.49, 4.46 , 0.5)
	MAPE	1.4	5.2	0.5
Double Hulthén	($S_{\ell 1}$, $S_{\ell 2}$, β, α, **a**)	(49.74, 36.61, 3.42, 2.82, 15.0)	(824.72, 737.18, 1.56, 0.12, 7.0)	(48.17, 1.33, 5.36, 4.14, 5.0)
	MAPE	3.2	5.4	1.2
MT	(V_R, V_A, μ, **a**)	(1189.46, 432.15, 0.46, 20.0)	(10737.19, 1527.78, 1.31, 8.0)	(952.66, 851.72, 1.01, 5.0)
	MAPE	2.7	4.7	1.3
Double exponential	(A, B, α_1, α_2, **a**)	(73.73, 14.53, 1.31, 0.59, 25.0)	(6381.90, 62.53, 4.50, 1.44, 9.0)	(55.51, 68.62, 3.08, 1.32, 4.0)
	MAPE	2.5	4.9	0.1

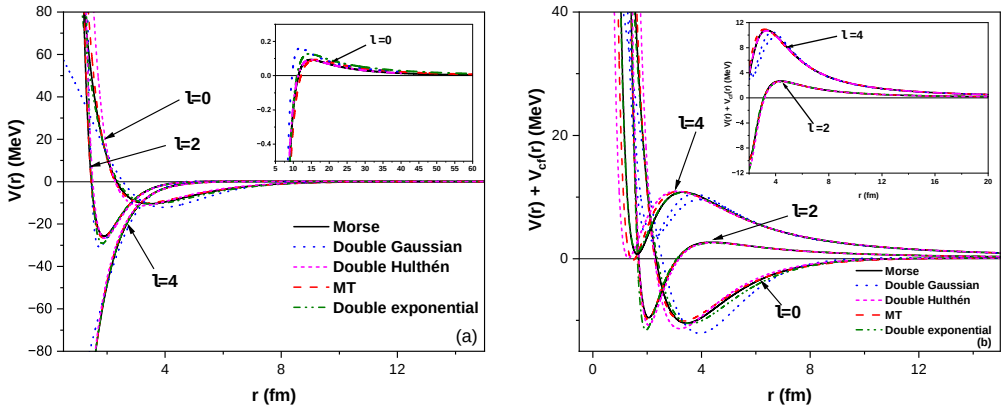

Figure 2. Interaction potentials without and with centrifugal potential $\ell = 0$, 2, and 4.

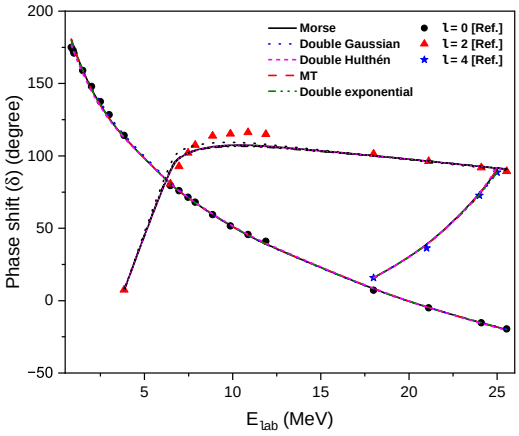

Figure 3. Obtained scattering phase shifts for $\ell = 0$, 2, and 4 along with expected phase shifts given in Ref. [10]

4. Conclusions

The optimized potentials for alpha-alpha scattering have been constructed by considering various successful models proposed for nuclear interactions, such as Morse, double Gaussian, double Hulthén Malfliet-Tjon, and double exponential functions with atomic Hulthén as ansatz for screened Coulomb interaction. The model parameters have been optimized using a global optimization algorithm [39] that minimizes mean absolute percentage error between the obtained scattering phase shifts from the phase function method and the experimental data. On comparison of the resultant optimized potentials, one can conclude that all the mathematical models agree with each other with small variations and with almost similar mean absolute percentage errors. Since the optimized potential approach utilizes all available experimental data, it provides a globally optimal solution that might become data-dependent. Hence, we have also performed optimization by considering only as many experimental data points as the number of model parameters. This procedure also lead to similar interaction potentials to those obtained using global optimization. Therefore, it is reasonable to conclude that all mathematical functions considered only serve to guide the process of obtaining the interaction potential and are not unique. This is going to be true for any potential as long as it has the basic required features of any two-body interaction, which are repulsion at short distances, attractive nature for intermediate distances, and exponentially falling of tail for large distances.

Acknowledgment

A. Awasthi acknowledges financial support provided by the Department of Science and Technology (DST), Government of India vide Grant No. DST/INSPIRE Fellowship/2020/IF200538.

References

[1] M. Sato, Y. Akaishi and H. Tanaka, "Phenomenological study of three-body force based on the energy levels of the alpha-particle," *Prog. Theor. Phys.* **66** (1981) 930-939. https://doi.org/10.1143/PTP.66.930

[2] D. M. Dennison, "Energy levels of the O^{16} nucleus," *Phys. Rev.* **96** (1954)378.

[3] L. Rosenfeld, "Nuclear Forces," *North-Holland Pub. Co. Interscience Publishers* (1948).

[4] E. Rutherford and J. Chadwick, "LII. The scattering of α particles by helium," *Phil. Mag. J. Sci.* **4** (1927) 605-620.

[5] N.P. Heydenburg and G.M. Temmer," Alpha-alpha scattering at low energies," *Phys. Rev.* **104** (1956) 123.

[6] T. A. Tombrello and L. S. Senhouse, "Elastic scattering of alpha particles from helium," *Phys. Rev.* **129** (1963) 2252.

[7] R. Nilson, W.K. Jentschke, G.R. Briggs, R. O. Kerman and J. N. Snyder, "Investigation of excited states in ^8Be by alpha-particle scattering from He," *Phys. Rev.* **109** (1958) 850.

[8] W.S. Chien and E.R. Brown, "Study of the $\alpha + \alpha$ system below 15 MeV (c.m.)," *Phys. Rev. C* **10** (1974) 1767.

[9] S.A. Afzal, A. A. Z. Ahmad and S. Ali, "Systematic Survey of the $\alpha - \alpha$ Interaction," *Rev. Mod. Phys.***41** (1969) 247.

[10] A. Khachi , L. Kumar and O.S.K.S Sastri, "Alpha–alpha scattering potentials for various-channels using phase function method," *Phys. At. Nucl.* **85** (2022) 382-391.

[11] P. Darriulat, G. Igo, H. G. Pugh and H.D. Holmgren, "Elastic scattering of alpha particles by helium between 53 and 120 MeV," *Phys. Rev.* **137** (1965) B315.

[12] S. Ali and A.R. Bodmer, "Phenomenological $\alpha - \alpha$ potentials", *Nucl. Phys.* **80** (1966) 99-112.

[13] B. Buck, H, Friedrich and C. Wheatley, "Local potential models for the scattering of complex nuclei", *Nucl. Phys. A* **275** (1997) 246-268.

[14] K. Wildermuth and W. McClure, "Cluster Representations of Nuclei", , *Berlin Heidelberg, Germany: Springer* (1966).

[15] S. Saito,"Interaction between clusters and Pauli principle," *Prog. Theor. Phys.* **41**(1969) 705–722.

[16] M. Odsuren K. Katō and M. Aikawa, "Scattering cross section for various potential systems," *Nucl. Data Sheets* **120** (2014) 126-128.

[17] A. Khachi, O.S.K.S Sastri, L.Kumar and A. Sharma, "Phase Shift Analysis for Alpha-alpha Elastic Scattering using Phase Function Method for Gaussian Local Potential," *J. Nucl. Phys. Mater. Sci. Radiat. Appl.*,**9** (2021) 1-5.

[18] A. Sharma, S. Gora, J. Bhagavathi and O.S.K.S. Sastri, "Simulation study of nuclear shell model using sine basis," *Am. J. Phys.* **88** (2020) 1-5.

[19] O.S.K.S Sastri, A. Khachi and L.Kumar, "An innovative approach to construct inverse potentials using variational Monte-Carlo and phase function method: application to np and pp scattering," *Braz. J. Phys.* **52** (2022) 58.

[20] M. Blažek ,"On a method for solving the inverse problem in potential scattering", *Comm. Math. Phys.***3** (1966) 282-291.

[21] S. Elhatisari, D. Le, G. Rupak et al. "Ab initio alpha–alpha scattering", *Nature* **528** (2015), 111–114

[22] S. Elhatisari, T.A.Lähde, D. Lee, U.G. Meißner and T. Vonk , "Alpha-alpha scattering in the Multiverse," *J. High Energ. Phys.*, **2** (2022), 1-30.

[23] J. Bhoi J and U. Laha, "Elastic scattering of light nuclei through a simple potential model," *Phys. At. Nucl.* **79** (2016) 370-374.

[24] J. Bhoi and U Laha, "Hulthén potential models for $\alpha - \alpha$ and $\alpha -^3 He$ elastic scattering," *Pramana* **88** (2017) 1-6.

[25] J. Bhoi, R. Upadhyay and U. Laha U. "Parameterization of Nuclear Hulthén Potential for Nucleus-Nucleus Elastic Scattering," *Commun. Theor. Phys.* **69** (2018) 203.

[26] L. Hulthen, "Uber die Eigenlösungen der Schrödinger- ¨ Gleichung des Deuterons", *Ark. Mat. Astron. Fys. A* **28** (1942) (in German).

[27] F. Ajzenberg-Selove, "Energy levels of light nuclei A = 5-10," *Nucl. Phys. A*, **490** (1988) 1-225.

[28] R.A. Malfliet , J.A. Tjon, "Solution of the Faddeev equations for the triton problem using local two-particle interactions," *Nucl. Phys. A*. **127**(1969) 1 161-8.

[29] H. Yukawa, S. Sakata, M. Kobayasi and M. Taketani, "On the interaction of elementary particles. IV," *Prog. Theor. Phys. Suppl.* **1** (1955) 46–71

[30] S. Awasthi, O.S.K.S. Sastri, "Real and imaginary phase shifts for nucleon-deuteron scattering using phase function method," *arXiv preprint arXiv:2304.10478*, 2023.

[31] P.M. Morse, "Diatomic molecules according to the wave mechanics. II. vibrational levels," *Phys. Rev.* **34** (1929) 57

[32] D.G. Yakovlev, M. Beard, L.R. Gasques and M. Wiescher, "Simple analytic model for astrophysical S-factors," *Phys. Rev. C***82** (2010) 044609.

[33] F Calogero, "Variable phase approach to potential scattering," *Academic, New York* (1967).

[34] B. Talukdar, D. Chatterjee and P. Banerjee, "A generalized approach to the phase-amplitude method," *J. Phys. G: Nucl. Phys.* **3** (1977) 813.

[35] G. C. Sett, U. Laha and B. Talukdar, "Journal of Physics A: Mathematical and General Phase-function method for Coulomb-distorted nuclear scattering," J. Phys. A: Math. Gen. **21** (1988) 3643.

[36] V.V.E. Babikov, "The phase-function method in quantum mechanics," *Sov. Phys. Uspekhi* **10** (1967) 271.

[37] G.J. Kynch , "The Two-Body Scattering Problem with Non-Central Forces I - Non-Relativistic," *Proc. Phys. Soc.* **65** (1952) 94

[38] D.R. Tilley, J. H. Kelley, J.L Godwin, D.J. Millener, J. E. Purcell , C. G. Sheu and H.R. Weller, "Energy levels of light nuclei A = 8,9,10," *Nucl. Phys. A* **745** (2004) 155-362.

[39] A. Khachi, L. Kumar, M.G. Kumar and O.S.K.S. Sastri, "Deuteron structure and form factors: Using an inverse potential approach," *Phys. Rev. C* **107** (2023) 064002.